Heterostructures of GaN with SiC and ZnO enhance carrier stability and separation in framework semiconductors

Matthew R. Farrow[*,1], John Buckeridge[**,1], Tomas Lazauskas[1], David Mora-Fonz[1], David O. Scanlon[1,2], C. Richard A. Catlow[1,3,4], Scott M. Woodley[1], and Alexey A. Sokol[1]

[1] Department of Chemistry, Kathleen Lonsdale Materials Chemistry, University College London, 20 Gordon Street, London WC1H 0AJ, UK
[2] Diamond Light Source Ltd., Diamond House, Harwell Science and Innovation Campus, Didcot, Oxfordshire OX11 0DE, UK
[3] The UK Catalysis Hub, Research Complex at Harwell, Rutherford Appleton Laboratory, Didcot OX11 0FA, UK
[4] Cardiff Catalysis Institute, School of Chemistry, Cardiff University, Main Building, Park Place, Cardiff CF10 3AT, UK

Keywords density functional theory, double bubbles, gallium nitride, photocatalysis, silicon carbide, zinc oxide

[*] Corresponding author: e-mail m.farrow@ucl.ac.uk, Phone: þ44 020 7679 0486
[**] e-mail j.buckeridge@ucl.ac.uk, Phone: þ44 020 7679 0486

A computational approach, using the density functional theory, is employed to describe the enhanced electron-hole stability and separation in a novel class of semiconducting composite materials, with the so-called double bubble structural motif, which can be used for photocatalytic applications. We examine the double bubble containing SiC mixed with either GaN or ZnO, as well as related motifs that prove to have low formation energies. We find that a 24-atom SiC sodalite cage inside a 96-atom ZnO cage possesses electronic properties that make this material suitable for solar radiation absorption applications. Surprisingly stable, the inverse structure, with ZnO inside SiC, was found to show a large deformation of the double bubble and a strong localisation of the photo-excited electron charge carriers, with the lowest band gap of ca. 2.15 eV of the composite materials considered. The nano-porous nature of these materials could indicate their suitability for thermoelectric applications.

1 **Introduction** One of the grand challenges in contemporary materials science is the one-step splitting of water into hydrogen and oxygen, using a single heterogeneous photocatalyst [1]. Photocatalysts, which typically operate by the separation of electron–hole pairs, traditionally are wide band-gap oxide semiconductors that operate in the UV-vis spectrum [2]. A promising photo-catalytic material that has recently been proposed is a solid solution of gallium nitride (GaN) and zinc oxide (ZnO) [3], which crystallises in the wurtzite structure and was shown to be able to achieve water splitting under visible light irradiation. Furthermore, to achieve a greatly enhanced efficiency, it is imperative to avoid the recombination of the photo-generated electron–hole pair.

Another major technological challenge is the fabrication of the p-type wide-gap semiconductors, which has been partially met for GaN but not for ZnO based transparent oxide materials [4, 5]. In contrast, SiC is widely used both as n- and p-type semiconductors. In fact, all three materials share a common structural motif based on a tetrahedral coordination of each atom, which results in simple lattices of wurtzite and zinc blende. Moreover, a large number of polytypes are also known for SiC, in which hexagonal one-atom thick layers (sheets) are stacked in differing patterns, with wurtzite (2H) and zinc blende (3R) being the most elementary examples. The bond lengths of SiC, ZnO and GaN are comparable, and, therefore, SiC can be readily exchanged into ZnO or GaN matrices, provided the charge balance is maintained. Further, SiC is one of the most mechanically and chemically stable materials, making it suitable for a plethora of applications and, importantly, it supports both electron and hole charge carriers [6].

In order to effect novel material properties, one of the current drivers in materials science, chemistry and physics is the search for novel nano-organised composite materials that combine the best features of two or more chemical compounds [7–12]. In this paper, we propose that, by combining SiC, ZnO and GaN, the resulting composite heterostructures will possess the ability to readily generate separable and stable electron–hole pairs. We build on our previous work, in which we have devised novel structures that comprise secondary building units (SBU) of 'perfect' 24-atom GaN, ZnO and SiC sodalite (b-) cages and 96-atom bubbles [13–15]. Cage-like molecular and extended structures including SiC have also been the topic of previous investigations [16, 17].

We organise the paper as follows. First, we provide the method, with which we construct these novel frameworks, and the computational details we have used are given. We then present the calculated electronic structure of the systems, and finish with a discussion of their viability in experimental work and potential applications.

2 Method

2.1 Construction of the systems We constructed our framework systems following the methodology outlined in our previous work [14, 15] as illustrated in Fig. 1. Three-dimensional tiling of polyhedral shapes can be achieved either by bonding or merging via corners (zero-dimensional), edges (one-dimensional) or faces (two-dimensional) [18]. Three types of structures are considered here. The first consists of a double-bubble framework, where a 12-atom sodalite cage is placed inside a 96-atom bubble to form the double bubble systems [19, 20]. The inner and outer bubbles can be either composed of the same compound or of different compounds, and we use the naming convention (AB)@(CD) to indicate that the compound AB moiety is inside the compound CD matrix. The second structural type is constructed from corner-sharing sodalite cages that, again, can be composed of the same compound or a structure formed by alternating two compounds. We term these systems LTA, adopting the standard zeolite nomenclature. The final structural type, which we call SOD, is formed by merging edge-sharing sodalite cages, and again the systems can be composed of one compound or two differing compounds.

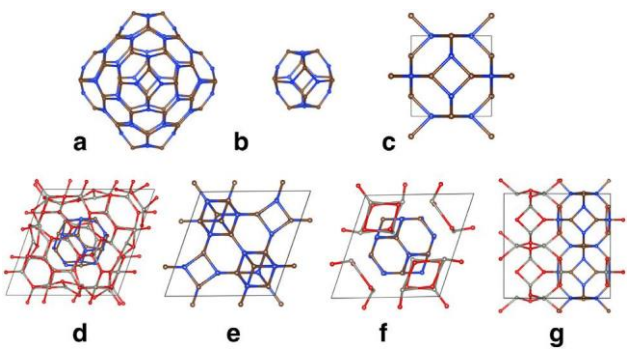

Figure 1 Secondary building units used to construct the framework systems. Where, a and b are the cage structures containing 96 and 24 atoms (the sodalite cage), respectively, c is the periodic sodalite structure, d is the periodic double bubble system, e and f are the LTA structures. g represents the SOD structure.

The ability to experimentally create these double bubble structures could be based on work on layered core–shell nanoparticles (and their composites) that are designed for quantum dots for the purpose of separating electrons and holes [21, 22]. Furthermore, the synthesis of microporous frameworks usually involves a template, which can be an organic molecule that helps to steer the nucleation towards the formation of cages, and these template molecules are, then, removed using post-synthetic treatments [23].

2.2 Computational details We employed the plane-wave density functional theory (DFT) code VASP [24–26] to determine the equilibrium structures and chose the solids-corrected Perdew-Burke-Ernzerhof (PBEsol) [27, 28] GGA exchange-correlation (XC) functional for the geometry optimisations. Within VASP, we used the projector augmented wave (PAW) method to describe the interactions between cores and the valence electrons [29], using four valence electrons for both silicon and carbon, thirteen for gallium, twelve for zinc, five for nitrogen and six for oxygen. An energy cut-off of 500 eV and a Monkhorst-Pack k-point mesh of 1 1 1 for the double bubble frameworks provided total energy convergence up to 10^{5} eV. Pure bulk phases of SiC, GaN and ZnO required k-point meshes of 8 8 6 for comparable total energy convergence. To avoid the problem of Pulay stress, each equilibrium structure was determined by optimising the atomic coordinates at a series of differing volumes and then fitting a Murnaghan equation of state to the resulting energy versus volume data. Furthermore, we performed single-point energy calculations at the hybrid level of theory using the PBEsol0 XC functional that includes 25% Hartree–Fock electron exchange. The electronic structure of the frameworks was characterised by computing their density of states (DOS) and partial DOS using PBEsol0. It is important to note that we have performed test geometry optimisations using the PBEsol0 XC functional, and found negligible changes in atomic structure. Therefore, we have used the PBEsol optimised geometries in single-point PBEsol0 calculations, to obtain the electronic structure characterisations.

2.3 The measure of stability The enthalpy of formation, H_f is calculated as:

$$H_f = \frac{E_{tot} - (n_1 E_a + n_2 E_b)}{n_1 + n_2}, \quad (1)$$

where E_{tot} is the total energy of the framework, E_a and E_b are the total energies of the pure bulk structures, and n_1 and n_2 are the numbers of formula units of each moiety, and, a and b represent SiC, GaN or ZnO.

3 Results

3.1 Atomic structure and stability The calculated radial distribution function (RDF) for a representative selection of systems containing SiC with GaN and ZnO can be seen in Fig. 2. From the plots, we see a close match between the sodalite cages of SiC and GaN for the SOD structure, and a slight mismatch for the LTA structure indicating that SiC and GaN are structurally similar. The double bubble systems again show how the SiC and GaN bond lengths are comparable. Curiously, a more pronounced mismatch in the structural parameters between the inner and outer bubbles for the structure SiC@ZnO results in a stronger deformation of the outer bubble compared to GaN@ZnO frameworks considered previously [14]. In this previous study, we found that the inner bubble is connected with the outer bubble via vertices to the faces of the outer bubble that are shared between three hexagons. Here, we have determined that $(SiC)_{12}@(ZnO)_{48}$ has a c2-3 structure (No. 5), whereas both $(SiC)_{12}@(GaN)_{48}$ and $(ZnO)_{12}@(SiC)_{48}$ possesses an fcc, orthorhombic structure, F222 (No. 22), although the latter breaks all symmetry constraints, probably due to the strongly incommensurate structure of

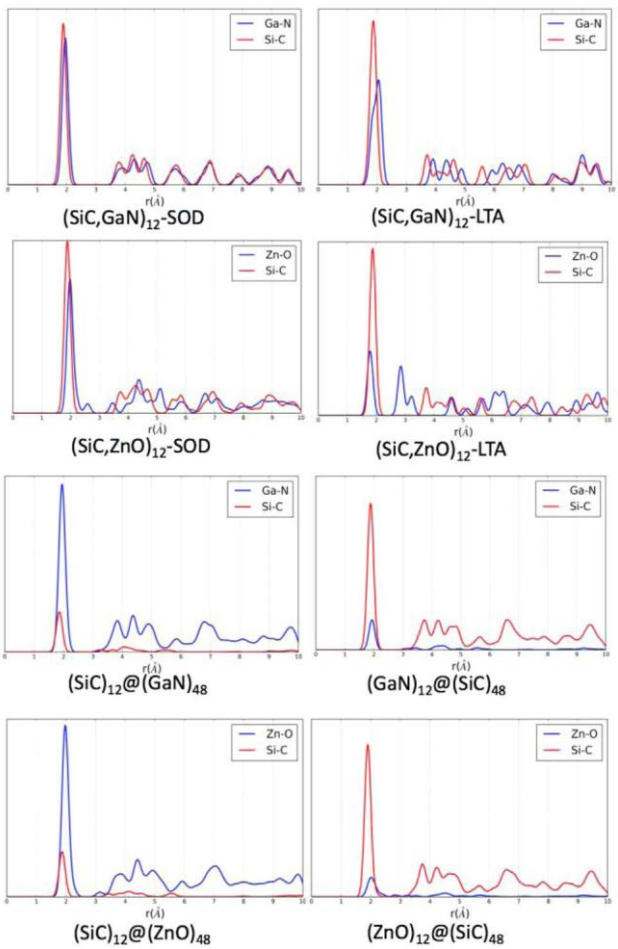

Figure 2 Radial distribution function plots for the framework systems comprising SiC, GaN and ZnO moieties.

the two moieties (see Fig. 3): The strong interactions between the inner and outer bubbles result in a fragmenta-tion of the inner bubble into six four-member rings (the hexagonal faces originally edge sharing to these tetragons expand). The surface of the outer bubble distorts in a similar way to isolated bubbles that are composed of strongly polarisable atoms; anions are slightly further out from the centre of the bubble than the cations. In our system, the silicon atoms are closer to the centre of its bubble by ca. 0.3 Å than carbon and, therefore, closer to the inner bubble, whereas the polarisation of the fragmented inner bubble is much smaller; Zn atoms are slightly further out by ca. 0.1 Å, which is the inverse of what we would expect for the isolated, non-fragmented $(ZnO)_{12}$ bubble. After the inner bubble expansion, bonding results between silicon and oxygen (ca. 1.75 Å)at the cost of elongating the Zn–O bonds between tetragonal faces, four of which are themselves slightly rotated about the axis that goes through the centre of the tetragonal face and the centre of the bubble. We note that the shortest Zn–C interatomic distances are approximately 2.0 Å,consistent with the zinc carbide structures. In summary, the outer bubble controls the binding between the inner and outer shells with the resulting structure of the inner bubble fragmenting and Zn ions moving further out than O ions, even if only slightly.

3.2 Electronic structure and charge carriers Table 1 summarises the calculated electronic band gaps of our semiconductor framework systems along with their standard enthalpy of formation with respect to the end member compounds (SiC, ZnO and GaN) in the

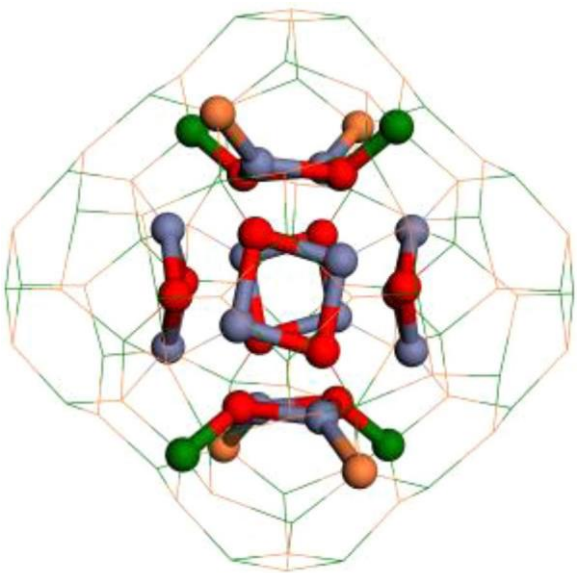

Figure 3 ZnO inner bubble (stick and ball model) showing the structural fragmentation inside a SiC bubble (line model). Sticks and ball are also employed to highlight bonding between the other bubble and just two of the six inner tetragons. (Red is reserved for oxygen, grey for zinc, green for silicon and copper for carbon).

Table 1 Band gap, E_g, and enthalpy of formation per formula unit, H_f, with respect to the end-member compounds, for the SiC, GaN and ZnO semiconductor frameworks, using the PBEsol0 density functional. For comparison, the corresponding values are given for pure SiC, GaN, and ZnO, in the wurtzite (2H) phase.

System	E_g (eV)	H_f (kJmol^{-1})
SiC	3.95	0.00
GaN	3.86	0.00
ZnO	3.07	0.00
$(SiC)_{12}$-SOD	3.45	51.92
$(SiC)_{12}$-LTA	3.62	86.65
$(SiC,GaN)_{12}$-SOD	3.94	80.38
$(SiC,GaN)_{12}$-LTA	4.75	136.97
$(GaN)_{12}@(SiC)_{48}$	3.83	65.53
$(SiC)_{12}@(GaN)_{48}$	2.90	61.34
$(SiC)_{12}@(ZnO)_{48}$	2.53	42.02
$(ZnO)_{12}@(SiC)_{48}$	2.14	49.02

wurtzite (2H) phase. The calculated partial density of states (pDOS) are given in Fig. 4. In pure end member compounds, as should be expected, the top of the valence band is dominated by carbon, nitrogen and oxygen states, whereas the bottom of the conduction is dominated by silicon, gallium and zinc states. The calculated values of the band gap of the three compounds are in good agreement with previous reports using similar methods (e.g. 3.90, 3.84 eV for SiC using B3LYP and PBE0 hybrid functionals using 25% exact exchange, respectively [30]; 3.23, 3.55 eV for GaN using HSE06 with 25 and 30% exact exchange, respectively [31]; and 3.14, 3.13 eV for ZnO using PBE0 and PBESol0, respectively [32]) and represent a marked improvement on simple local or gradient corrected density functional approximations (e.g. 2.05, 2.11, 2.29 eV for SiC using LDA [33, 34] and PBE GGA [35], respectively; 1.86, 2.58 for GaN using a PBE GGA, and PBE þ U [36], respectively; 0.75 eV, 1.83 eV for ZnO using PW91 GGA and GGA þ U, respectively [37]). Our results are still typically deviate from experiment (cf. Fig. 5) to within ca. 10%, which can be related to an unbiased non-empirical character of the hybrid PBESol0 density functional employed; with a marked contrast between the band-gap overestimation for SiC and GaN and underestimation for ZnO. A further improvement should be expected from quasiparticle calculations using Green's function methods, which are however still not feasible for the framework materials with large unit cells.

To understand the fundamental driving forces in the observed pDOS of the heterogeneous systems (shown in Fig. 4), we refer the reader to the band alignment of the respective bulk phases illustrated in Fig. 5, which also provides experimental values of the band gap in these materials. As is clear from Fig. 5, the ionisation potentials decrease as the anion species moves from group 16 to group 14 and similarly, the electron affinities decrease with the same trend. The majority of these nanoporous systems obey the same trends as their pure end-member counterparts. Although, notably, $(SiC,GaN)_{12}$-LTA breaks this trend by having a much larger band gap than the other nanoporous systems. This is probably due to the changes in Madelung potential for the atoms in the very porous LTA structure [38].

As previously found by our group [39], the SiC sodalite is a stable low-energy polymorph, which is stabilised further in the $(SiC)_{12}@(ZnO)_{48}$ double bubble system. The much lower energy gap (2.5 eV) makes this system a candidate for solar radiation absorption applications that do not depend on electron mobility (cf. Table 2).

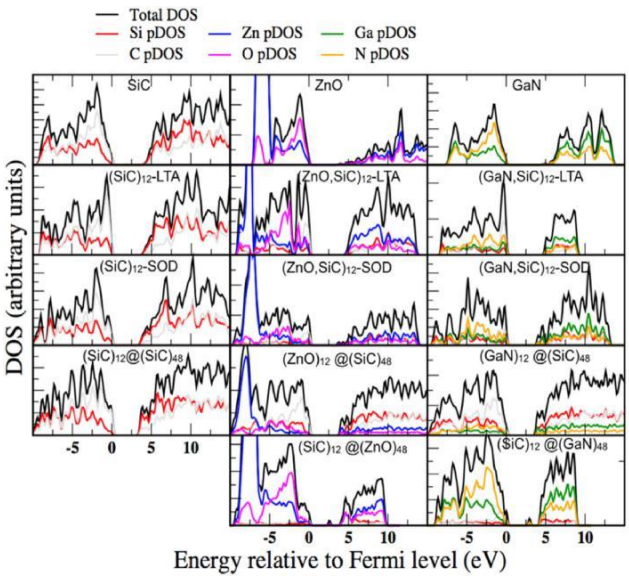

Figure 4 Total and partial Density of States (pDOS) plots for the novel framework systems.

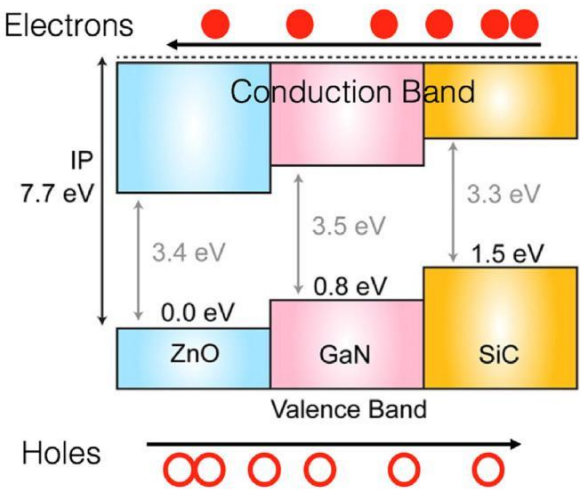

Figure 5 Calculated bulk band alignment of the wurtzite (2H) phases of SiC, GaN and ZnO using available experimental band gap values [40]. Adapted from Figure 1 in [6].

Table 2 Calculated electron and hole effective masses of the wurtzite and double bubble systems (experimental data for effective masses are taken as geometric averages over the tensor components). Calculated electron and hole effective masses of the wurtzite and double bubble systems (bold) along with experimen-tal data that are taken as geometric averages over the principal tensor components. Values are given in units of electron mass.

system	m_e	m_h
ZnO	0.23,0.22[a],0.24[b]	1.29,0.93[c],1.47[d]
GaN	0.20,0.19[a],0.20[c]	2.06,0.80[e],1.44[a],2.2[f]
SiC	0.26,0.49[g], 0.29[h]	2.07,1.0[g]
$(SiC)_{12}@(GaN)_{48}$	0.28	10.87
$(SiC)_{12}@(ZnO)_{48}$	0.37	1.31
$(ZnO)_{12}@(SiC)_{48}$	1.18	0.86

[a]exp. [45]; [b]exp. [46]; [c]exp. [47]; [d]exp. [48]; [e]exp. [49, 50]; [f]exp. [51]; [g]exp. (SiC-6H) [52]; [h]exp. (SiC-4H) [53].

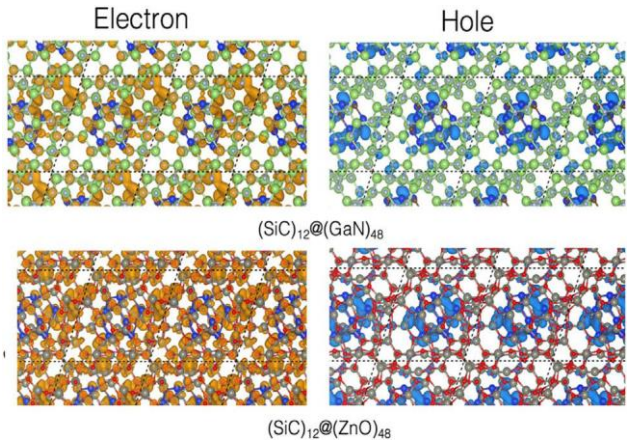

Figure 6 Electron (orange) and hole (blue) iso-surfaces for the double bubble frameworks of SiC@GaN/ZnO.

The relatively high effective masses are common to all bubble systems considered, which does, however, limit the range of potential applications.

The calculated standard enthalpy of formation (H_f) for the double-bubble, SOD, and LTA structures is roughly comparable with that of fullerenes with respect to bulk carbon (ca. 40 kJ mol ^{1}) [41]. Furthermore, the alternative nanoporous SiC framework material with the LTA architecture has a higher enthalpy of formation (by ca. 35 kJ/mol per formula unit), but still is thermodynamically plausible: one can envisage potential routes to its synthesis using pore-filling templates.

Unexpectedly, out of all systems considered, $(ZnO)_{12}@(SiC)_{48}$ which we term here as scanlonia, possesses the smallest band gap of 2.14 eV and one of the lowest enthalpies of formation (49 kJ/mol). The heavy charge carrier masses of scanlonia (see Table 2) would make this material if synthesised an ideal candidate for a solar light radiation collector for optical applications, for example, as a pigment.

Additionally, it is known that nanoporous solids often display lower thermal conductivities than their dense counterparts, which points to possible applications in thermoelectrics. To realise this potential application, an understanding of the defect physics (especially, the response of the system to dopants) is a prerequisite (e.g. [42]), which is beyond the scope of this initial screening.

The calculated isotropic effective masses for ground-state wurtzite polymorphs and selected double bubble systems are summarised in Table 2 along with the available experimental data. We find excellent agreement between our values and experiment apart from the hole effective mass for SiC. The reliability of the experimental data for holes in 2H–SiC is quite low, but we can compare our value of 2.07 with 2.05, which has been obtained from theoretical LDA data of Lambrecht et al. [43] (not including spin-orbit splitting). Interestingly, inclusion of spin-orbit effects results in a significantly lower value of 0.83 corroborated by a later report of 0.81 [44]. The overall close agreement still gives us confidence in our prediction for the composite materials, but also highlights the need for a careful re-examination of spin-orbit effects on effective masses in this class of material.

The double bubble effective masses prove to be competitive with those of the ground state systems. Notably, the $(SiC)_{12}@(GaN)_{48}$ system has the highest asymmetry with the m_h/m_e of 38 compared to the value of 2 for SiC (6H). For all three double bubble systems, the hole resides on the SiC moiety (see Fig. 6) and the electron is localised on its counterpart. When SiC is the inner bubble in the system, m_h/m_e is greater than unity, and the transport is dominated by the lighter electron carriers. Conversely, when SiC is the outer bubble, the hole dominated mobility will prove to be low. The clear electron–hole separation and the strong asymmetry in these charge carrier masses forms a good basis for prospective photocatalytic, optoelectronic and more generally, energy materials applications.

4 Conclusions The addition of a wide gap semiconducting material SiC to the family of heterogeneous framework materials has led to the formulation of a new composite semiconductor with enhanced stability of hole charge carriers and improved potential for electron-hole separation. We find that these materials have quite large electron and hole effective masses and therefore, are perhaps more suited to solar radiation collectors, with optical applications for pigmentation, for example. These composite frameworks may also have the potential to be possible thermoelectric materials, although further investigations with respect to their defect physics are required. To ascertain the stability of these materials, further investiga-tion into their mechanical and dynamical properties is necessary.

The proposed class of novel semiconducting materials are both mechanically robust and energetically accessible

and therefore, the challenge of realising these materials is now in the experimental domain.

Acknowledgements

We thank our colleagues Matthew B. Watkins, Stephen A. Shevlin, Arunabhiram Chutia and Dominic Chaopradith whose work provided impetus to the current development. The EPSRC is acknowledged for funding for: Matthew R. Farrow on grant number EP/K038419; Tomas Lazauskas and Scott M. Woodley on grant numbers EP/ I03014X and EP/K038958; John Buckeridge on grant number EP/K016288. Computational resources were provided though the Materials Chemistry Consortium on grant number EP/L000202.

References

[1] A. Fujishima and K. Honda, Nature 238, 37 (1972).
[2] A. Kudo and Y. Miseki, Chem. Soc. Rev. 38, 253 (2009).
[3] K. Maeda, T. Takata, M. Hara, N. Saito, Y. Inoue, H. Kobayashi, and K. Domen, J. Am. Chem. Soc. 127, 8286–8287 (2005).
[4] J. Buckeridge, C. R. A. Catlow, D. O. Scanlon, T. W. Keal, P. Sherwood, M. Miskufova, A. Walsh, S. M. Woodley, and A. A. Sokol, Phys. Rev. Lett. 114, 016405 (2015).
[5] J. Buckeridge, C. R. A. Catlow, D. O. Scanlon, T. W. Keal, P. Sherwood, M. Miskufova, A. Walsh, S. M. Woodley, and A. A. Sokol, Phys. Rev. Lett. 115, 029702 (2015).
[6] A. Walsh, J. Buckeridge, C. R. A. Catlow, A. J. Jackson, T. W. Keal, M. Miskufova, P. Sherwood, S. A. Shevlin, M. B. Watkins, S. M. Woodley, and A. A. Sokol, Chem. Mater. 25, 2924–2926 (2013).
[7] R. Wu, B. Zha, L. Wang, K. Zhou, and Y. Pan, Phys. Status Solidi A 209, 553–558 (2012).
[8] M. Niu, F. Huang, L. Cui, P. Huang, Y. Yu, and Y. Wang, ACS Nano 4, 681–688 (2010).
[9] W. Li, Q. Jia, X. Liu, and J. Zhang, Ceram. Int. 43, 2950–2955 (2017).
[10] Y. Wang, Y. Wang, E. Hosono, K. Wang, and H. Zhou, Angew. Chem. Int. Ed. 47, 7461–7465 (2008).
[11] S. Dey, M. D. Hossain, R. A. Mayanovic, R. Wirth, and R. A. Gordon, J. Mater. Sci. 52, 2066–2076 (2017).
[12] W. Zhao, Y. Liu, Z. Wei, S. Yang, H. He, and C. Sun, Appl. Catal. B 185, 242–252 (2016).
[13] A. A. Sokol, M. R. Farrow, J. Buckeridge, A. J. Logsdail, C. R. A. Catlow, D. O. Scanlon, and S. M. Woodley, Phys. Chem. Chem. Phys. 16, 21098–21105 (2014).
[14] M. Farrow, J. Buckeridge, C. Catlow, A. Logsdail, D. Scanlon, A. Sokol, and S. Woodley, Inorganics 2, 248 (2014).
[15] M. R. Farrow, C. R. A. Catlow, A. A. Sokol, and S. M. Woodley, Mater. Sci. Semicond. Process. 42(Part 1), 147–149 (2016).
[16] A. V. Pokropivny and S. Volz, J. Mater. Sci. 48, 2953–2960 (2013).
[17] P. Melinon, SiC Cage Like Based Materials, in: Silicon Carbide – Materials, Processing and Applications in Electronic Devices, edited by M. Mukherjee InTech, DOI: 10.5772/21861.
[18] S. M. Woodley, M. B. Watkins, A. A. Sokol, S. A. Shevlin, and C. R. A. Catlow, Phys. Chem. Chem. Phys. 11, 3176–3185 (2009).
[19] S. Hamad, C. R. A. Catlow, E. Spano, J. M. Matxain, and J. M. Ugalde, J. Phys. Chem. B 109, 2703–2709 (2005).
[20] C. R. A. Catlow, S. T. Bromley, S. Hamad, M. Mora-Fonz, A. A. Sokol, and S. M. Woodley, Phys. Chem. Chem. Phys. 12, 786–811 (2010).
[21] B. O. Dabbousi, J. Rodriguez-Viejo, F. V. Mikulec, J. R. Heine, H. Mattoussi, R. Ober, K. F. Jensen, and M. G. Bawendi, J. Phys. Chem. B 101, 9463–9475 (1997).
[22] R. Ghosh Chaudhuri and S. Paria, Chem. Rev. 112, 2373–2433 (2012).
[23] J. H. Jung, H. Kobayashi, K. J. C. van Bommel, S. Shinkai, and T. Shimizu, Chem. Mater. 14, 1445–1447 (2002).
[24] G. Kresse and J. Hafner, Phys. Rev. B 47, 558–561 (1993).
[25] G. Kresse and J. Hafner, Phys. Rev. B 49, 14251–14269 (1994).
[26] G. Kresse and J. Furthm€uller, Comput. Mater. Sci. 6, 15–50 (1996).
[27] J. P. Perdew, K. Burke, and M. Ernzerhof, Phys. Rev. Lett. 77, 3865 (1996).
[28] J. P. Perdew, A. Ruzsinszky, G. I. Csonka, O. A. Vydrov, G. E. Scuseria, L. A. Constantin, X. Zhou, and K. Burke, Phys. Rev. Lett. 100, 136406–136404 (2008).
[29] P. E. Bl€ochl, Phys. Rev. B 50, 17953 (1994).
[30] T. Oda, Y. Zhang, and W. J. Weber, Chem. Phys. Lett. 579, 58–63 (2013).
[31] P. G. Moses, M. Miao, Q. Yan, and C. G. V. d. Walle, J. Chem. Phys. 134, 084703 (2011).
[32] D. Mora-Fonz, J. Buckeridge, A. J. Logsdail, D. O. Scanlon, A. A. Sokol, S. Woodley, and C. R. A. Catlow, J. Phys. Chem. C 119, 11598–11611 (2015).
[33] C. H. Park, B.-H. Cheong, K.-H. Lee, and K. J. Chang, Phys. Rev. B 49, 4485–4493 (1994).
[34] C. Persson, and U. Lindefelt, Phys. Rev. B 54, 10257–10260 (1996).
[35] S. Jakub, P. Jacek, Ł. Michał, and K. Stanisław, New J. Phys. 12, 043024 (2010).
[36] Z. Wang, M. Zhao, X. Wang, Y. Xi, X. He, X. Liu, and S. Yan, Phys. Chem. Chem. Phys. 14, 15693–15698 (2012).
[37] P. Erhart, K. Albe, and A. Klein, Phys. Rev. B 73, 205203 (2006).
[38] J. Buckeridge, K. T. Butler, C. R. A. Catlow, A. J. Logsdail, D. O. Scanlon, S. A. Shevlin, S. M. Woodley, A. A. Sokol, and A. Walsh, Chem. Mater. 27, 3844–3851 (2015).
[39] M. B. Watkins, S. A. Shevlin, A. A. Sokol, B. Slater, C. R. A. Catlow, and S. M. Woodley, Phys. Chem. Chem. Phys. 11, 3186–3200 (2009).
[40] O. Madelung, Semiconductors: Data Handbook (Springer, Berlin Heidelberg 2004).
[41] R. F. Curl and R. C. Haddon, Phil. Trans. R. Soc. A 343, 19–32 (1993).
[42] Z. Xie, Y. Sui, J. Buckeridge, C. R. A. Catlow, T. W. Keal, P. Sherwood, A. Walsh, D. O. Scanlon, S. M. Woodley, and A. A. Sokol, Phys. Status Solidi A (2016) DOI: 10.1002/pssa.201600445
[43] W. R. L. Lambrecht, S. Limpijumnong, S. N. Rashkeev, and B. Segall, Phys. Status Solidi B 202, 5–33 (1997).
[44] C. Persson and U. Lindefelt, J. Appl. Phys. 86, 5036–5039 (1999).
[45] T. Hanada, Oxide and nitride semiconductors: Processing, properties, and applications, in: Basic Properties of ZnO, GaN, and Related Materials, edited by T. Yao and S.-K. Hong (Springer, Berlin, Heidelberg, 2009) pp. 1–19.
[46] R. L. Weiher, Phys. Rev. 152, 736–739 (1966).

[47] W. R. L. Lambrecht, A. V. Rodina, S. Limpijumnong, B. Segall, and B. K. Meyer, Phys. Rev. B 65, 075207 (2002).

[48] S. L. Shi and S. J. Xu, J. Appl. Phys. 109, 053510 (2011).

[49] J. I. Pankove, Optical properties of GaN, RCA Rev. 36, 163–176 (1975).

[50] V. Bougrov, M. E. Levinshtein, S. L. Rumyantsev, and A. Zubrilov, Properties of Advanced SemiconductorMaterials GaN, AlN, InN, BN, SiC, SiGe (John Wiley & Sons, New York, 2001).

[51] J. S. Im, A. Moritz, F. Steuber, V. H€arle, F. Scholz, and A. Hangleiter, Appl. Phys. Lett. 70, 631–633 (1997).

[52] N. T. Son, O. Kordina, A. O. Konstantinov, W. M. Chen, E. Sörman, B. Monemar, and E. Janzén, Appl. Phys. Lett. 65, 3209–3209 (1994).

[53] N. T. Son, W. M. Chen, O. Kordina, A. O. Konstantinov, B. Monemar, E. M. Janzen, D. Hofman, D. Volm, M. Drechsler, B. K. Meyer, A. O. Konstantinov, B Monemar, E. Janze, and D. M. Hofman, Appl. Phys. Lett. 66, 1074–1074 (1995).